Title
Geranylgeranylated-chlorophyll-protein complexes in lhl3 mutant of the green alga Chlamydomonas reinhardtii

Journal
The Plant Journal, 120(4)

ISSN
0960-7412

Authors
Kodru, Sireesha
Nellaepalli, Sreedhar
Ozawa, Shin-Ichiro
et al.

Publication Date
2024-11-01

DOI
10.1111/tpj.17071

the plant journal

SEB SOCIETY FOR EXPERIMENTAL BIOLOGY

The Plant Journal (2024) **120,** 1577–1590 doi: 10.1111/tpj.17071

Geranylgeranylated-chlorophyll-protein complexes in *lhl3* mutant of the green alga *Chlamydomonas reinhardtii*

Sireesha Kodru[1,2,†,‡], Sreedhar Nellaepalli[1,2,*,†,‡], Shin-Ichiro Ozawa[1,2,3], Chihiro Satoh[1,2], Hiroshi Kuroda[1,2], Ryouichi Tanaka[4], Katharine Guan[5], Marilyn Kobayashi[5,6], Phoi Tran[5], Sarah McCarthy[5], Setsuko Wakao[5,7], Krishna K. Niyogi[5,6,7,8] and Yuichiro Takahashi[1,2,*]

[1]*Research Institute for Interdisciplinary Science, Okayama University, 3-1-1 Tsushima-naka, Kita-ku, Okayama 700-8530, Japan,*

[2]*JST-CREST, Tokyo, Japan,*

[3]*Institute of Plant Science and Resources, Okayama University, Okayama, Japan,*

[4]*Institute of Low Temperature Science, Hokkaido University, Sapporo, Japan,*

[5]*Department of Plant and Microbial Biology, University of California, Berkeley, California 94720, USA,*

[6]*Howard Hughes Medical Institute, University of California, Berkeley, California 94720, USA,*

[7]*Molecular Biophysics and Integrated Bioimaging Division, Lawrence Berkeley National Laboratory, Berkeley, California 94720, USA,*

[8]*Innovative Genomics Institute, University of California, Berkeley, California 94720, USA*

Received 3 May 2024; revised 4 September 2024; accepted 25 September 2024; published online 15 October 2024.
*For correspondence (e-mail taka@cc.okayama-u.ac.jp and sreedhar.nellaepalli@biology.ox.ac.uk).
†These authors contributed equally to this work.
‡Present address: Section of Molecular Plant Biology, Department of Biology, University of Oxford, Oxford, UK

SUMMARY

Chlorophylls *a* and *b* (Chl *a* and *b*) are involved in light harvesting, photochemical reactions, and electron transfer reactions in plants and green algae. The core complexes of the photosystems (PSI and PSII) associate with Chl *a*, while the peripheral antenna complexes (LHCI and LHCII) bind Chls *a* and *b*. One of the final steps of Chl biosynthesis is the conversion of geranylgeranylated Chls ($Chls_{GG}$) to phytylated Chls by geranylgeranyl reductase (GGR). Here, we isolated and characterized a pale green mutant of the green alga *Chlamydomonas reinhardtii* that was very photosensitive and was unable to grow photoautotrophically. This mutant has a 16-bp deletion in the *LHL3* gene, which resulted in the loss of LHL3 and GGR and accumulated only $Chls_{GG}$. The *lhl3* mutant cells grown in the dark accumulated PSII and PSI proteins at 25–50% of WT levels, lacked PSII activity, and retained a decreased PSI activity. The PSII and PSI proteins were depleted to trace amounts in the mutant cells grown in light. In contrast, the accumulation of LHCI and LHCII was unaffected except for LHCA3. Our results suggest that the replacement of Chls with $Chls_{GG}$ strongly affects the structural and functional integrity of PSII and PSI complexes but their associating LHC complexes to a lesser extent. Affinity purification of HA-tagged LHL3 confirmed the formation of a stable LHL3-GGR complex, which is vital for GGR stability. The LHL3-GGR complex contained a small amount of PSI complex assembly factors, suggesting a putative coupling between Chl synthesis and PSI complex assembly.

Keywords: photosynthesis, photosystem, pale-green mutant, chlorophyll-protein complex, geranylgeranyl reductase.

INTRODUCTION

Chlorophylls *a* and *b* (Chl *a* and Chl *b*), which associate with chlorophyll-binding proteins to form chlorophyll-protein complexes, are pivotal in the photosynthesis of algae and plants. The photosystems I and II (PSI and PSII) core complex consisting of reaction center (RC) and core antennae bind a number of Chl *a* molecules, which are involved in light harvesting and photochemical reactions (Ben-Shem et al., 2003; Jensen et al., 2003; Jordan et al., 2001; Nelson & Yocum, 2006; Suga et al., 2019; Wei et al., 2016; Zouni et al., 2001). In contrast, light-harvesting complexes (LHCs) associate with both Chl *a* and Chl *b* and play a role in light absorption, excitation energy transfer, and thermal dissipation (Ben-Shem et al., 2003; Liu et al., 2004; Qin et al., 2015; Su et al., 2017; Suga et al., 2019). These chlorophyll-protein complexes often

associate with each other to form supercomplexes in the thylakoid membranes of oxygenic photosynthetic organisms.

Chl *a* and Chl *b* molecules are composed of chlorophyllide and phytol moieties, which are synthesized via the tetrapyrrole and isoprenoid biosynthesis pathways, respectively, by a cascade of enzymes in cyanobacteria and chloroplasts (Moulin & Smith, 2005; Porra & Grimme, 1978; Rudiger, 1997; Tanaka & Tanaka, 2007). Phytol moieties of the Chls are derived from geranylgeranyl pyrophosphate (GGPP). During the final steps of chlorophyll biosynthesis, geranylgeranyl reductase (GGR) encoded by the *CHLP* gene catalyzes the reduction (hydrogenation) of geranylgeranyl pyrophosphate (GGPP) to phytyl pyrophosphate (PhyPP) via dihydrogeranylgeranyl pyrophosphate (DHGGPP) and tetrahydrogeranylgeranyl pyrophosphate (THGGPP). In this catalysis, the double bonds in GGPP are sequentially hydrogenated (Rudiger et al., 1998; Shpilyov et al., 2005) (Figure S1). Chl synthase esterifies either GGPP or PhyPP to chlorophyllide generating geranylgeranylated Chls ($Chls_{GG}$) and mature phytylated Chls, respectively (Beale, 1990; Moulin & Smith, 2005). The three successive hydrogenation steps of the side chain of $Chls_{GG}$ to phytol of the mature Chls are also catalyzed by GGR via dihydrogeranylgeranylated Chls (Chl_{DHGG}) and tetrahydrogeranylgeranylated Chls (Chl_{THGG}) (Rudiger et al., 1998; Shpilyov et al., 2005). In the green lineage, Chl *b and* Chl b_{GG} are produced from Chl *a* and Chl a_{GG}, respectively, by chlorophyll *a* oxygenase (CAO) (Tanaka et al., 1998; von Wettstein et al., 1995). In addition to Chl biosynthesis, GGR activity is also crucial in α-tocopherol and phylloquinone synthesis (Tanaka et al., 1999, 2010).

A *chlP* mutant of the cyanobacterium, *Synechocystis* sp. PCC 6803 deficient in GGR accumulates Chl a_{GG} and α--tocotrienol instead of Chl *a* and α-tocopherol, respectively, and is unable to grow photoautotrophically (Shpilyov et al., 2005). Transgenic tobacco plants expressing a reduced amount of GGR showed defects in chlorophyll and tocopherol biosynthesis and displayed phenotypes of pale green, light sensitivity, and stunted growth (Tanaka et al., 1999). In the green lineage, the light-harvesting-like protein 3 (LIL3) with two putative transmembrane helices and an Lhc motif stabilizes GGR, playing essential roles in chlorophyll and tocopherol biosynthesis in *Arabidopsis thaliana* (Lohscheider et al., 2015; Tanaka et al., 2010). *A. thaliana* has two isoforms, LIL3:1 and LIL3:2, which are functionally redundant. A double mutant defective in *lil3:1* and *lil3:2* is significantly affected in the stability and function of GGR (Lohscheider et al., 2015; Tanaka et al., 2010). In *Oryza sativa*, a double mutant defective in *lil3* and *chlp* accumulated $Chls_{GG}$ and displayed a lethal phenotype (Li et al., 2019). In *Chlamydomonas reinhardtii*, one light-harvesting-like protein 3 (*LHL3*) gene, which is ortholog of the *LIL3* gene in *A. thaliana*, has been identified (Teramoto et al., 2004).

The phytyl tail moiety is structurally more flexible than the geranylgeranyl tail moiety, because the former contains one double bond while the latter contains four double bonds. Because the phytyl chains are located in the hydrophobic regions of chlorophyll-binding proteins, the rigid structure of the geranylgeranyl tail moiety may significantly affect the assembly, function, and structure of chlorophyll-protein complexes. The occurrence of PSI and PSII complexes was revealed by measuring fluorescence spectra at 77K in *Synechocystis* sp. PCC 6803 and rice mutants deficient in GGR (Li et al., 2019; Shpilyov et al., 2005). The cyanobacterial mutant showed a decreased PSII activity, and PSI may be functional (Shpilyov et al., 2005). Accordingly, it remains to be investigated further the effects of the replacement of Chls by $Chls_{GG}$ on biochemical structure of chorophyll-protein complexes and the activities of PSI and PSII.

In this study, we analyzed a pale-green mutant of the green alga *C. reinhardtii*, which accumulated only geranylgeranylated Chls and was unable to grow photoautotrophically. This mutant lacks both GGR and LHL3 and has a wild-type (WT) *GGR* gene but a 16-bp deletion in the *LHL3* gene. We characterized the function and structure of the geranylgeranylated-chlorophyll-protein complexes accumulated in the *lhl3* mutant cells and found that the PSII and PSI complexes are assembled, but their stability is severely impaired in the light. PSI showed a reduced photochemical reaction, whereas PSII was inactive. However, the geranylgeranylated-chlorophylls-containing LHC complexes were mostly stable in the *lhl3* mutant. Moreover, biochemical purification of the GGR-LHL3 complex from an HA-tagged transgenic line, *lhl3*/LHL3-HA, showed an interaction with PSI assembly factors, raising the possibility of their transient association during the biogenesis of chlorophyll-protein complexes.

RESULTS

Isolation of a pale-green mutant accumulating geranylgeranylated chlorophylls

Several pale-green mutants that are deficient in light-harvesting complexes (LHCIs and LHCIIs) and grow photoautotrophically have been reported in the green alga *C. reinhardtii* (Bujaldon et al., 2017, 2020; Devitry & Wollman, 1988; Michel et al., 1983; Picaud & Dubertret, 1986). Here, we describe a pale-green mutant of *C. reinhardtii* that is photosensitive and unable to grow photoautotrophically (Dent et al., 2005). The mutant cells grew heterotrophically on solid TAP medium supplemented with acetate in the dark and showed a pale-green phenotype (Figure 1a). The growth of the mutant cells was significantly

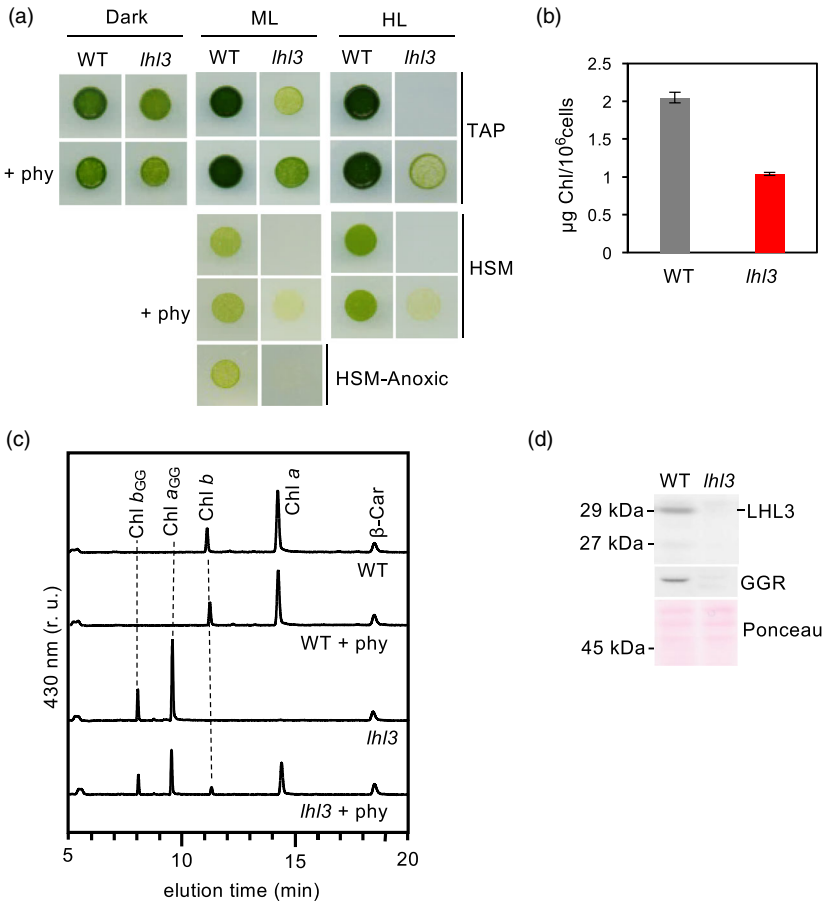

Figure 1. The *lhl3* mutant is defective in LHL3 and GGR accumulation.
(a) Cells grown in the dark in liquid TAP medium were spotted on to solid TAP or HSM medium and exposed to different light intensities (ML, 30 μmol photons m^{-2} sec^{-1}; HL, 200 μmol photons m^{-2} sec^{-1}). +phy, presence of exogenous supply of 1 μM phytol on solid medium. Cell growth under anoxic conditions (no oxygen and 20% CO_2) was tested on solid HSM medium.
(b) Chlorophyll quantification. Cells were grown under dim light (DL, 2–5 μmol photons m^{-2} sec^{-1}). Data are presented as the means ± SD (n = 3).
(c) Detection of Chl *a*, Chl *b*, Chl a_{GG}, and Chl b_{GG} by HPLC. Pigments of cells grown under DL were extracted with DMF and were separated on C18 reverse column and were assigned based on their retention times.
(d) Accumulation of LHL3 and GGR was determined by immunoblotting. Nitrocellulose membrane was stained with ponceau S.

suppressed under medium light (ML, 30 μmol photons m^{-2} sec^{-1}) and was inhibited under high light (HL, 200 μmol photons m^{-2} sec^{-1}) (Figure 1a). The mutant cells were unable to grow photoautotrophically on minimal medium (HSM) under ML and HL conditions. It is reported that the photoautotrophic growth of the *cgl71* mutant, which lacks one of PSI complex assembly factors, CGL71, is impaired in ambient conditions but is restored under anoxic conditions (Heinnickel et al., 2016; Nellaepalli et al., 2021). However, the *lhl3* mutant did not grow photoautotrophically (Figure 1a). These observations suggest that the mutant cells are highly photosensitive or are photosynthetically nonfunctional.

The pale-green phenotype of the mutant was confirmed by measuring cellular chlorophyll content by spectrophotometry. The mutant cells contained half of the chlorophyll per cell compared with WT cells (Figure 1b). We subsequently extracted pigments from cells grown under dim-light conditions (DL, 2–5 μmol photons m^{-2} sec^{-1}) and analyzed them by high-performance liquid chromatography (HPLC). Chl *a* and Chl *b* were detected in WT as expected (Figure 1c). In contrast, the mutant cells contained no detectable Chl *a* and Chl *b* but accumulated geranylgeranylated chlorophylls (Chl a_{GG} and Chl b_{GG}). This indicates that the mutant cells are deficient in the reduction by GGR of the geranylgeranyl side chain of $Chls_{GG}$ to phytyl side chain or of geranylgeranyl pyrophosphate to phytyl pyrophosphate (Figure S1). When the culture media were supplemented with phytol, the photosensitivity of the mutant growth on TAP medium was relieved, and the photoautotrophic growth on HSM medium was partially recovered (Figure 1a). In extracts from the mutant cells supplemented with exogenous phytol, Chl *a* and Chl *b* were detected although their amounts were lower than in the extracts of WT cells (Figure 1c). These results indicate that the phytol added in the media was used for the synthesis of phytylated chlorophylls from the chlorophyllides in the mutant cells, although phytol is very hydrophobic (Figure S1).

To detect the presence of GGR in the mutant, total cellular proteins were analyzed by immunoblotting using an anti-GGR antibody (Figure 1d). GGR was not detectable in the mutant, which is consistent with the pigment analysis data. It has been reported that LIL3 plays a role in binding GGR to the thylakoid membranes in Arabidopsis (Takahashi et al., 2014). The immunoblot with an anti-LHL3 antibody revealed that LHL3, which is encoded in an ortholog of the *LIL3* gene in *Chlamydomonas*, was absent from the

mutant (Figure 1d). This phenotype could result from a mutation in either the *GGR* or *LHL3* gene of *C. reinhardtii*.

Pale-green mutant has a mutation in *LHL3*

Backcrosses of the pale-green mutant to WT revealed a 2:2 segregation of the growth phenotype in 20 tetrads, suggesting that there is a single nuclear mutation that is responsible for the phenotype. Next, we amplified the *GGR* gene and found no mutation in the mutant compared to WT. Then, we sequenced LHL3 mRNA by RT-PCR and found a 16-bp deletion in exon1 (E1) (Figure 2a; Table S2). Amplification of the E1 region with genomic DNA as a template revealed that the size of the amplified DNA fragment of the mutant (120-bp) is 16-bp smaller than that of the WT DNA fragment (136-bp) (Figure 2b).

To confirm that mutation of the *LHL3* gene is responsible for the phenotype, the mutant cells were complemented with an expression vector containing the genomic *LHL3* DNA by nuclear transformation as described in "Materials and Methods" section. Immunoblotting revealed that the complemented strains accumulated LHL3 and GGR proteins nearly at WT levels (Figure 2c). Pigment analysis showed that the complemented strains accumulated Chl *a* and Chl *b* like WT but no detectable level of $Chls_{GG}$ (Figure 2d). It is concluded that the absence of LHL3 protein results in the instability of GGR in the mutant cells, as LHL3 likely anchors GGR to the thylakoid membranes as LIL3 does in Arabidopsis (Takahashi et al., 2014). Therefore, we designate the pale-green mutant as *lhl3* mutant in the following sections. LHL3 consists of two putative transmembrane domains and an LHC-motif and is an ortholog of LIL3 of higher plants (Figure S2).

Activities of PSI and PSII in *lhl3* mutant cells

The inability of the *lhl3* mutant to grow photosynthetically was characterized by measuring the light-induced Chl fluorescence induction kinetics (Figure 3a). WT cells exhibited a normal fluorescence induction kinetics, whereas the mutant cells showed no variable fluorescence. The absence of PSII activity was also confirmed by measuring the O_2 evolution in the presence of 0.3 mM 2,6-dichlorobenzoquinone (DCBQ) as an artificial electron acceptor, and no activity was detected in the *lhl3* mutant cells (Figure 3b). When the *lhl3* cells grew in the presence of phytol, partial restoration of PSII activities was detected. These results indicated that phytylated-Chl *a* is essential for the PSII function. Then, the PSI activity was measured using a Joliot-type spectrophotometer. The *lhl3* cells exhibited P700 photooxidation activity at ~20% of WT levels (Figure 3c). This indicates that Chl a_{GG} can substitute for the PSI photochemical reaction at a lower efficiency. The photoautotrophic growth of the mutant cells was partially restored when the cells were grown in the presence of phytol (Figure 1a). The PSII and PSI activities on Chls basis were recovered to ~30 and ~75% of WT levels, respectively, in the presence of phytol (Figure 3b,c). Thus, the recovered photoautotrophic growth of the *lhl3* cells

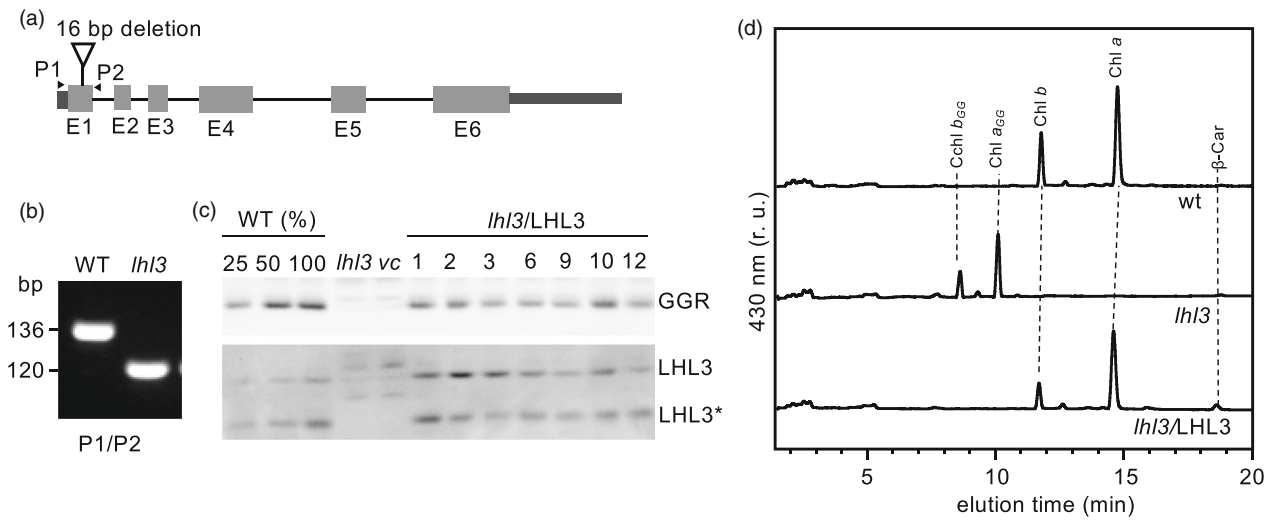

Figure 2. Identification of mutation in *LHL3* and mapping of the deletion site in *lhl3* mutant.
(a) Schematic representation of *LHL3* gene (Cre03.g199535) in *Chlamydomonas reinhardtii*. The deletion of 16 bp in the *LHL3* gene of the *lhl3* mutant is indicated. Gray boxes indicate the exons, and the lines indicate introns. P1 and P2 denote forward and reverse primers (#16/#17 and #15/#18, respectively).
(b) PCR analysis with *lhl3*-specific primers yields a PCR product of 136 bp product in WT and 120 bp product in the *lhl3* mutant indicating a 16 bp deletion.
(c) Accumulation of GGR and LHL3 by immunoblotting in WT, *lhl3*, and complemented strains (Clones, 1, 2, 3, 6, 9, 10, 12). LHL3*, proteolytic fragment; vc, vector control.
(d) HPLC chromatography to detect Chl *a*, Chl *b*, Chl a_{GG}, and Chl b_{GG}.

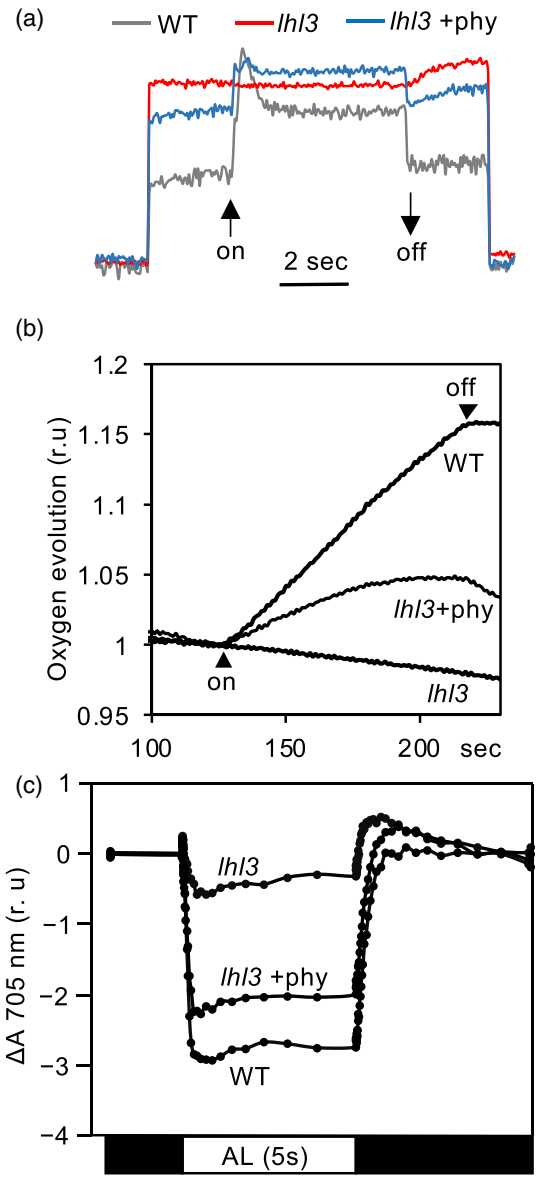

Figure 3. PSII and PSI activities in WT and *lhl3* mutant.
(a) Chl *a* fluorescence kinetics measured with a Dual-PAM.
(b) Kinetics of oxygen evolution activity measured in cells in the presence of DCBQ as an electron acceptor.
(c) Redox activities of P700 in cells in the presence of inhibitors (DCMU/DBMIB). AL, actinic light.

when phytol was added in the growth medium results from the partial recovery of PSI and PSII activities.

Chl_{GG} destabilizes PSI and PSII complexes

To examine the accumulation of PSI and PSII proteins in the *lhl3* cells, total cellular proteins from WT and *lhl3* cells grown under dark and medium light (ML) conditions were analyzed by immunoblotting (Figure 4a). When the cells were grown in the dark, immunoblotting with antibodies against proteins in PSI (PsaA, PSAD, and PSAL) and PSII (PsbA and PsbC) showed that the *lhl3* mutant cells accumulated PSI and PSII proteins at ~50 and ~25% of WT levels, respectively. When the cells were grown under ML conditions, PSII and PSI core proteins in *lhl3* cells were further reduced to 10–15% of WT levels, indicating that both photosystems are sensitive to light. Upon the addition of phytol in the growth medium, the accumulation of PSI and PSII core subunits was restored nearly to WT levels in dark-grown *lhl3* mutant cells. However in mutant cells grown in ML, the PSII proteins accumulated less, whereas PSI proteins accumulated similarly to that of WT cells (Figure 4a).

The accumulation of the peripheral antenna proteins of PSI and PSII (LHCIs and LHCIIs) was determined by immunoblotting. In contrast to the PSI and PSII core proteins, the amount of the LHCII proteins was not significantly affected in the *lhl3* mutant cells grown in the dark and ML (Figure 4b). The level of some LHCI proteins varied in the *lhl3* mutant cells to some extent. The accumulation of LHCA3 decreased in the dark and became undetectable in ML (Figure 4c). LHCA9 increased in the dark but remained unchanged in ML. LHCA2 and LHCA7 decreased, whereas LHCA1, LHCA4, and LHCA6 increased in ML. The decrease in LHCA7 in ML may be caused by the lack of LHCA3 because they have an intimately interaction (Moseley et al., 2002; Ozawa et al., 2018; Suga et al., 2019). The levels of LHCA5 and LHCA8 are the least affected.

To assess the stability of chlorophyll-binding proteins containing of $Chls_{GG}$, cells were incubated in the presence of an inhibitor of chloroplast translation, chloramphenicol (CHL), or cytoplasmic translation, cycloheximide (CHX), and then the stability of the chlorophyll-binding proteins was analyzed. The dark-grown WT and *lhl3* cells were shifted to the ML growth condition after the addition of the inhibitor, and an equal amount of cell culture was analyzed during the time course of 6 h. In the WT cells, the chloroplast-encoded PsaA and PsbA protein levels remained stable. It is known that PSII turns over rapidly under strong light conditions, but PsbA scarcely degraded under ML conditions. In the *lhl3* cells, however, PSI and PSII subunits decreased in abundance over time (Figure 4d). PSAD, a nucleus-encoded stromal PSI subunit, which is destabilized in the absence of PSI reaction center (RC) subunits (Takahashi et al., 1991), was gradually lost in the mutant cells, whereas nucleus-encoded LHCA8 was stably maintained in both WT and *lhl3* mutant cells. These results reveal that the stability of the core complexes associating with Chl a_{GG} is impaired when compared to the LHCA8 complex associating with Chl a_{GG} and Chl b_{GG}. It is noted that LHCA3 was unstable in the *lhl3* mutant, like the PSI core complex, which is consistent with previous observations in a PSI-deficient mutant (Naumann et al., 2005; Takahashi et al., 2004).

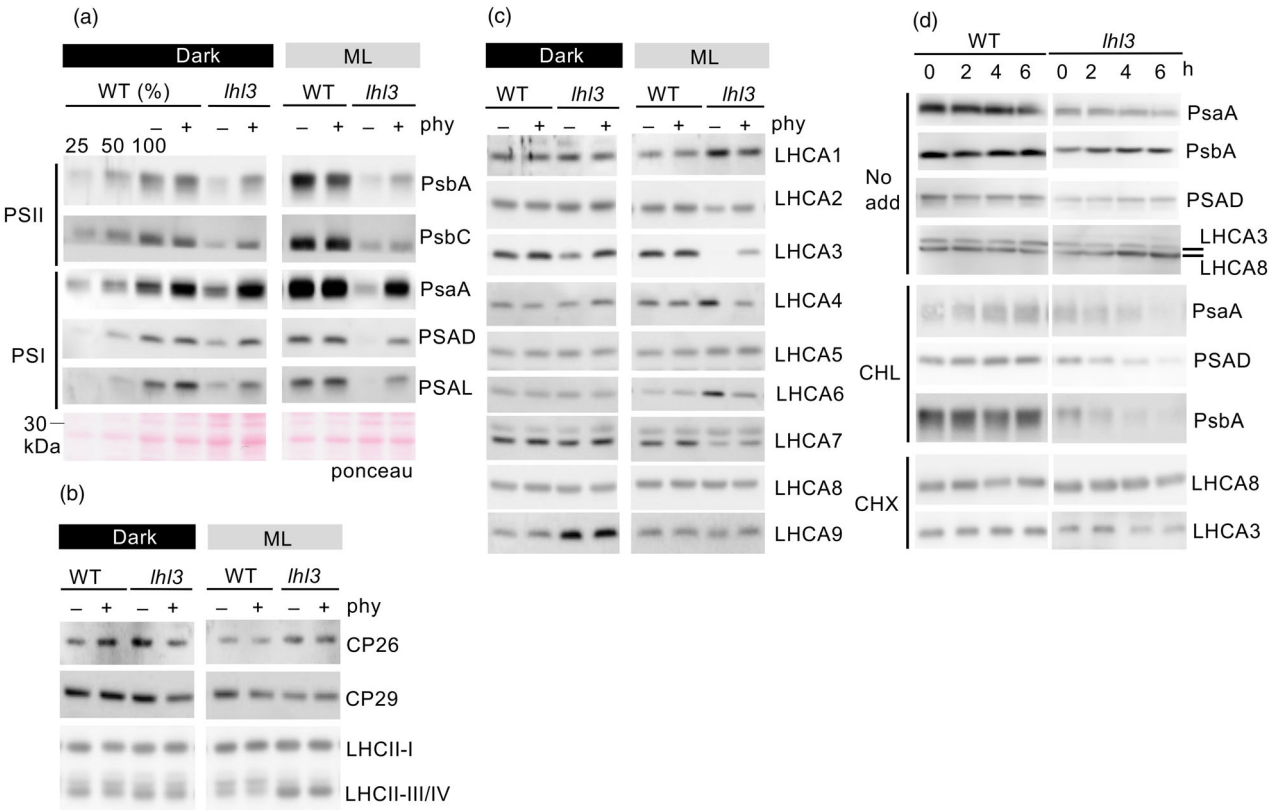

Figure 4. Accumulation of chlorophyll-binding proteins in WT and *lhl3* mutant.
(a) Immunoblotting with antibodies against PSII and PSI subunits. Nitrocellulose membrane was stained with Ponceau S. Total cellular proteins from WT and *lhl3* grown under dark and light conditions (ML) on equal chlorophyll basis were separated by SDS-PAGE.
(b) Immunoblotting with antibodies against LHCII subunits.
(c) Immunoblotting with antibodies against LHCI subunits.
(d) Stability of PSI and LHCI subunits. Cells were incubated in the absence of inhibitors (No add) or in the presence of 100 μg mL^{-1} chloramphenicol (CHL) or 100 μg mL^{-1} cycloheximide (CHX) to monitor the stability of chloroplast-encoded subunits (PsaA and PsbA) or nucleus-encoded subunits (LHCA3 and LHCA8) by immunoblotting. The stability of nucleus-encoded subunit, PSAD, was also monitored in the presence of chloramphenicol.
Samples were analyzed based on equal chlorophyll (a–c). For stability assay (d), samples were normalized based on equal chlorophylls before incubating with the inhibitors and for each time point equal volume of the samples was analyzed.

$Chls_{GG}$-binding protein complexes

To investigate the effects of the presence of $Chls_{GG}$ on the organization of pigment-protein complexes, these complexes were separated by sucrose density gradient ultracentrifugation from thylakoid membrane extracts solubilized with 1% β-DDM (Figure 5). As already reported (Nellaepalli et al., 2021; Takahashi et al., 2006), pigment-protein complexes of WT were mainly resolved in three distinct green bands, A1 (LHCII), A2 (PSII core), and A3 (PSI-LHCI). The separation pattern of chlorophyll-protein complexes of the *lhl3* cells grown in the dark was similar to that in WT although the amount of A3 (PSI-LHCI) decreased (Figure 5a). A2 from WT cells was devoid of PSI and LHCI proteins (Figure 5c). In contrast, A2 from the mutant contained both PSII proteins (PsbA and PsbC) and PSI proteins (PsaA and PSAD) as well as LHCI proteins (Figure 5c). It remains to be addressed whether PSI-LHCI and dissociated PSI core and LHCI oligomer exist *in vivo* or the solubilization partially dissociates unstable PSI-LHCI into PSI core and LHCI oligomer. This indicates that more PSI core and LHCI oligomers are present in A2 of the mutant than of WT, implying that the association between PSI core and LHCI oligomer is less stable in the mutant. Although the accumulation of the PSII RC protein (PsbA) was markedly decreased as shown in Figure 4(a), the PSII proteins form a PSII core complex. When the mutant cells were grown in the presence of phytol, the amount of the PSI-LHCI in A3 increased. The amount of A2 did not change, which indicates that the increased level of PSII proteins (PsbA and PsbC) and the decreased amount of PSI and LHCI proteins in A2 is a result of stabilization of PSI-LHCI supercomplex.

When the *lhl3* cells were grown under ML conditions, the PSI proteins (PsaA, PSAD, PSAL, and PSAG) were lost from A2 and A3 (Figure 5b,d), as expected from the results shown in Figure 4(a). This confirms that the PSI complex is

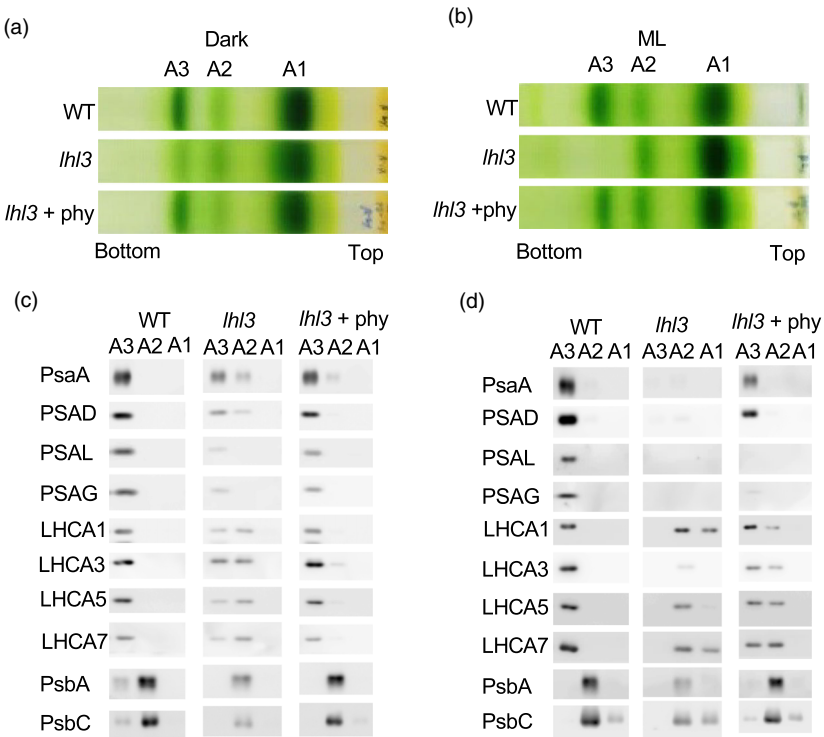

Figure 5. Separation and identification of chlorophyll protein complexes in WT and *Ihl3* mutant. (a, b) Thylakoid membranes were solubilized with 1.0% (w/v) β-DM, and the extracts were separated by sucrose density gradient ultracentrifugation. Cells were grown in either dark (a, c) or ML (b, d). (c, d) Immuno-detection of the polypeptides in A1, A2, and A3 fractions of WT and *Ihl3*.

degraded, whereas LHCI oligomer was stable in the *Ihl3* mutant under the ML condition. PSII (PsbA and PsbC) is still present in A2 fraction in the mutant. Although LHCA3 was not detected in total cellular proteins of the *Ihl3* mutant cells grown in ML, a faint signal was detected in A2 together with LHCA7, suggesting that they are still part of LHCI oligomers. It is inferred that PSI core complex is markedly more light-sensitive than the PSII core complex in the *Ihl3* mutant cells. Upon addition of phytol in the growth medium, the accumulation of PSI-LHCI in A3 was restored under ML conditions (Figure 5d).

LHL3 and GGR form a complex

The absence of LHL3 destabilized GGR, as shown in Figure 1, so we hypothesized an interaction between LHL3 and GGR. To analyze this interaction by pull-down experiments, the *Ihl3* mutant was complemented with a vector expressing an HA-tagged LHL3 protein (*LHL3-HA*). Photoautotrophic growth and accumulation of LHL3 and GGR proteins of three complemented *Ihl3*/*LHL3-HA* clones are shown (Figure 6a,b). LHL3-HA was expressed only at 10–30% of WT levels in the three clones of *Ihl3*/LHL3-HA, suggesting that the insertion of the HA tag at the C-terminus of LHL3 decreases the stability of LHL3 or suppresses the expression of the *LHL3* gene. The complemented strains accumulated the PSII reaction center subunit PsbA at substantial levels. This suggests that the amount of LHL3-HA is a minimum level for the restoration of PSII proteins and photoautotrophic growth. Among the complemented strains, the restoration of PsbA accumulation in clone 46 was better than in the other clones, which is consistent with the faster photoautotrophic growth of this clone (Figure 6a). These results indicate that accumulation of LHL3 and GGR, even at reduced amounts compared to WT, significantly stabilizes PSII complexes but does not fully restore its function and photoautotrophic growth (Figure 6a). The pigment elution profile by HPLC revealed that the amount of Chls *a* and *b* of *Ihl3*/*LHL3* was similar to that of WT (Figure 2d), but the *Ihl3*/*LHL3-HA* accumulated $Chls_{DHGG}$, $Chls_{THGG}$, and $Chls_{GG}$ to certain levels, because this complemented strain contains a decreased amount of GGR (Figure 6c). Since GGR successively hydrogenates $Chls_{GG}$ to phytylated-Chls via $Chls_{DHGG}$ and $Chls_{THGG}$, the low levels of GGR in the *Ihl3* mutant resulted in the accumulation of $Chls_{DHGG}$ and $Chls_{THGG}$ to certain levels.

Thylakoid membranes from WT and *Ihl3*/*LHL3-HA* were isolated and solubilized with 1% α-DDM, and the resulting extracts were applied to affinity purification spin-columns. The polypeptides from the eluted samples were separated by SDS-PAGE and visualized by staining with flamingo fluorescent dye (Figure 7a). LHL3-HA and GGR were detected in the LHL3-HA preparation, whereas only non-specific faint bands around 67 kDa were detected in WT. LC–MS/MS analysis of silver-stained polypeptides also indicated the enrichment of GGR and LHL3 proteins in the LHL3-HA preparation. Several minor polypeptides (F1-ATPase, Chlamyopsin, LHCA1, and UMP synthase) were detected in trace amounts in the LHL3-HA preparation

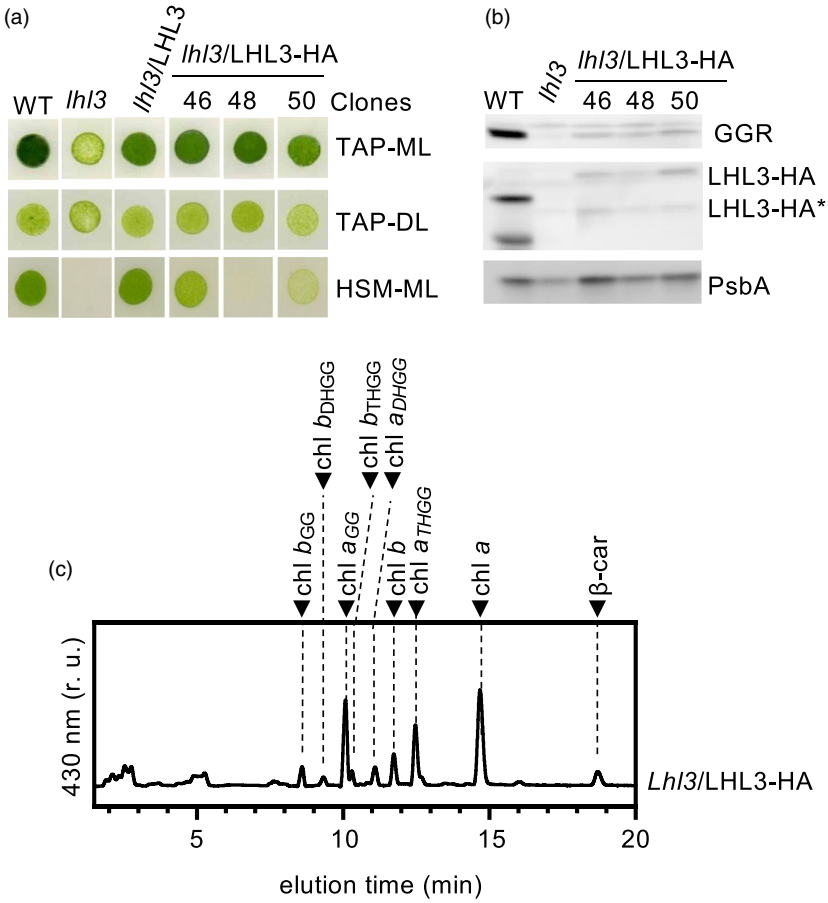

Figure 6. HA-tagged LHL3 transgenic lines.
(a) The growth of WT, *lhl3* and complemented strains, *lhl3*/LHL3, and *lhl3*/LHL3-HA (clone 46, 48, and 50), under photoheterotrophic (TAP-ML and TAP-DL) and photoautotrophic conditions (HSM-ML).
(b) Accumulation of GGR, LHL3, and PsbA proteins was analyzed by immunoblotting. LHL3*, proteolytic fragment.
(c) Separation of pigments extracted from *lhl3*/LHL3-HA cells (clone 46) with an HPLC.

(Figure S5), but we concluded that they are non-specifically interacting contaminations (Figure S3; Table S3). These results indicate that LHL3-HA stably interacts with GGR.

To determine the size of the GGR-LHL3 complex, the affinity-purified LHL3-HA was fractionated by sucrose density gradient ultracentrifugation (Figure S4a). Also, pigment-protein complexes from solubilized WT thylakoid membranes were separated by Blue-Native polyacrylamide gel electrophoresis (Figure S4b). LHL3 and GGR were fractionated between LHCII trimer (~120 kDa) and PSII core dimer (~340 kDa) and were separated at a size larger than 242 kDa. According to the apparent size, it is possible that a dimer of LHL3 associates with a dimer of GGR as reported in Arabidopsis (Takahashi et al., 2014).

GGR-LHL3 complex has a weak interaction with PSI assembly factors

During the assembly of chlorophyll-protein complexes, it is expected that apoprotein integration into the thylakoid membranes is coupled with pigment insertion into the apoproteins. Thus, it is possible that the interaction of LHL3-GGR affects insertion of chlorophyll into chlorophyll-binding apoproteins such as components of PSI, PSII, and LHCPs, because the reduction of geranylgeranylated chlorophylls to synthesize phytylated chlorophylls is one of the last steps of the chlorophyll synthesis. We detected neither PSI nor PSII proteins but a small amount of Ycf3 and Ycf4, which are assembly factors for PSI complex, in the LHL3-GGR complex by immunoblotting (Figure 7b). Since the amount of Ycf3 and Ycf4 proteins was below the level of detection by staining, it is necessary to confirm whether Ycf3 and Ycf4 preparations obtained by affinity purification contain GGR and LHL3 (Nellaepalli et al., 2018) (Figure S4). Immunoblot analyses showed that both preparations contain small amounts of LHL3 and GGR (Figure 7c,d). These results suggest that the GGR-LHL3 complex may have transient physical associations with the assembly machinery of PSI complex and that the assembly of PSI complex is intimately coupled with the synthesis of chlorophylls.

DISCUSSION

Chlamydomonas *lhl3* mutant lacks LHL3-GGR and accumulates $Chls_{GG}$

In the present study, we analyzed the pale-green mutant, *lhl3*, in which *LHL3* gene has a 16-bp deletion. Pigment analysis revealed that the *lhl3* mutant cells accumulate

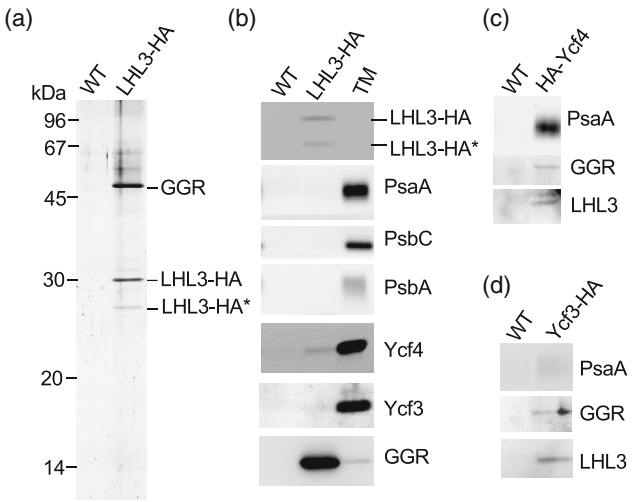

Figure 7. GGR-LHL3 complex transiently interacts with PSI assembly factors.
(a) LHL3-HA preparation affinity purified from thylakoid extracts solubilized with 1% α-DDM from *lhl3*/LHL3-HA (clone 46) and WT.
(b) Immunoblotting with antibodies against LHL3, GGR, PsaA, PsbA, PsbC (CP43), Ycf4, and Ycf3. LHL3-HA*, proteolytic fragment.
(c) Immunoblotting of polypeptides of HA-Ycf4 affinity purified from thylakoid extracts solubilized with 1% β-DDM from HA-ycf4 strains.
(d) Immunoblotting of polypeptides of affinity purified Ycf3-HA from thylakoid extracts solubilized with 1% α-DDM from ycf3-HA strain. TM, thylakoid membranes.

exclusively geranylgeranylated Chls ($Chls_{GG}$) and no phytylated Chls, indicating that the mutant cells lack geranylgeranyl reductase (GGR) activity. Immunoblotting showed that both LHL3 and GGR proteins are absent from the mutant cells. Genetic complementation of the mutant with a WT copy of the *LHL3* gene recovered the accumulation of both LHL3 and GGR and that of phytylated Chls, confirming that the phenotype is due to the mutation in the *LHL3* gene (Figure 2d). This result is consistent with the phenotypes of the *lil3* mutants of vascular plants, *A. thaliana* and *O. sativa* (Li et al., 2019; Takahashi et al., 2014). Since affinity purification of LHL3-HA copurified GGR, we conclude that LHL3 and GGR form a stable complex. Thus, LHL3 stabilizes GGR and is functionally required for chlorophyll biosynthesis similar to LIL3 in Arabidopsis (Tanaka et al., 2010). The *Chlamydomonas lhl3* mutant provides an additional advantage to study the effect of the replacement of phytylated Chls by geranylgeranylated Chls on the function and stability of chlorophyll-binding protein complexes such as PSI, PSII and LHCs, because of the ability of *Chlamydomonas* to grow on acetate as a carbon source.

Chl a_{GG} is not functional for PSII reaction and is inefficient for PSI reaction

The PSII core complex binds 35 Chl *a* molecules, with the core antenna complexes, CP43 and CP47, binding 13 and 16 Chl *a* molecules, respectively, whereas the reaction center (RC) complex, consisting of D1 (PsbA) and D2 (PsbD) heterodimer, associates with six Chl *a* molecules (Shen et al., 2019; Sheng et al., 2019; Umena et al., 2011). The PSI core complex associates with about 100 Chl *a* molecules, in which most Chl *a* molecules bind to two homologous reaction center subunits, PsaA and PsaB, while several Chl *a* molecules bind to peripheral subunits such as PsaF, PsaG, PsaH, PsaI, PsaJ, PsaK, and PsaL (Ben-Shem et al., 2003; Su et al., 2019; Suga et al., 2019). Thus, it is interesting to analyze whether PSI and PSII core complexes are assembled and stabilized in the *lhl3* mutant cells. The presence of PSI and PSII complexes containing Chl a_{GG} was investigated by measuring low temperature fluorescence spectra in S*ynechocystis* mutants deficient in ChlP (GGR) in which Chl a_{GG} accumulates instead of Chl *a* (Shpilyov et al., 2005, 2013). They discussed the stability of PSI and PSII based on the fluorescence spectra at 77K. To understand the effects of the deficiency of the phytol moieties on photosynthetic apparatus, it remains to be addressed to analyze the PSI and PSII protein levels and the complex formation.

Chlamydomonas lhl3 mutant cells accumulated a small amount of PSII complex but exhibited no oxygen evolution (Figure 3). The presence of a PSII core complex in the mutant reveals that Chl a_{GG}-containing PSII core complex is assembled but is functionally inactive. Since the primary electron donor, P680, is a Chl *a* dimer and the accessory chlorophylls are monomeric Chls *a*, and the intermediate electron acceptor is a pheophytin *a* (Pheo *a*), it is concluded that Chl *a* and/or Pheo *a* are essential for PSII functionality. Although Chl a_{GG} and/or Pheo a_{GG} do not substitute for the function of Chl *a* and/or Pheo *a*, it remains unclear which redox component(s) is nonfunctional for PSII activity. It is known that the PSII complex is stable but turns over rapidly in the light. The present study

showed that the accumulation of the PSII complex containing Chl a_{GG} is decreased under ML conditions where WT PSII complex is stable, indicating that the PSII complex containing Chl a_{GG} is more prone to photodamage. It is reported that the absence of GGR would halt the conversion of α-tocotrienols to α-tocopherols, which are involved in protecting PSII from photoinhibition (Inoue et al., 2011). However, it was reported that α-tocopherol is not required for PSII to protect it from photodamage (Maeda & Della-Penna, 2007; Shpilyov et al., 2013), but it cannot be excluded that the light-induced destabilization of PSII is partly ascribed to the absence of α-tocopherol.

The *lhl3* mutant cells accumulated a low amount of PSI complex. According to the activity of P700 photooxidation shown in Figure 3(b), the PSI complex containing Chl a_{GG} was active. The redox components of PSI are the primary electron donor P700, which consists of Chl *a* and Chl *a* epimer (Chl *a*′), and two monomeric accessory Chls *a*. These Chls *a* can be functionally replaced by Chls a_{GG} in an inefficient manner. In contrast to PSII, PSI is stable under strong light conditions in the WT cells. However, PSI complexes containing Chl a_{GG} in the *lhl3* mutant cells were as unstable as PSII complexes containing Chl a_{GG} (Figure 4d).

Decreased accumulation of PSI and PSII complexes in the *lhl3* mutant cells can be ascribed to the structure of the geranylgeranyl side chain in Chl a_{GG} molecules. The phytol side chain of Chl *a* contains only one double bond and is structurally flexible, whereas the geranylgeranyl side chain of Chl a_{GG} has four double bonds making the structure of the side chain rigid. Since the side chains of Chl *a* fit in hydrophobic regions of the binding proteins to be stabilized (Ben-Shem et al., 2003; Jordan et al., 2001; Qin et al., 2015; Su et al., 2019; Suga et al., 2019), the geranylgeranyl side chains may not fit in the binding pockets properly. PSI and PSII core complexes bind ~100 and 35 Chl *a* molecules, respectively, and the structural perturbations caused by binding Chl a_{GG} may induce the destabilization. It is also possible that the photochemical reactions occurring in Chl a_{GG} of PSI and PSII may generate side reactions such as reactive oxygen species and cause stronger photoinhibition to PSI and PSII complexes. However, the cell growth was not restored under anoxic conditions (Figure 1a).

It is of interest that the addition of hydrophobic phytol to the culture media markedly restored the accumulation of PSI and PSII complexes (Figures 4 and 5). Only part of geranylgeranylated Chls is converted to phytylated Chls because a small amount of added hydrophobic phytol may be dissolved in the growth medium. These observations suggest that the stability of the PSI and PSII complexes in the mutant cells is induced by partial replacement of geranylgeranylated Chl *a* by phytylated Chl *a*. However, the photosensitivity was not fully recovered by the partial replacement. It can be speculated that precise functional structures of the PSI and PSII must be pivotal for excitation energy transfer in the core antenna complexes and/or photochemical reactions to protect the reaction centers from damage by light.

Chls$_{GG}$-containing LHC complexes are stable

In contrast to the PSI and PSII core complexes, trimeric and monomeric LHCIIs binding Chls$_{GG}$ were stable under dark and light conditions (Figure 4b). Although these LHCII proteins each bind 12–14 Chls *a* and *b* molecules at fixed positions, it is likely that the rigid structure of the geranylgeranyl side chain of Chls$_{GG}$ did not significantly affect the stable structure. Most of the LHCIs binding Chls$_{GG}$ were relatively stable under dark and light conditions, whereas LHCA3 and LHCA7 were unstable in the light (Figure 4c,d). The PSI core associates with ten LHCIs in *Chlamydomonas* (Ozawa et al., 2018). Two layers of tetrameric LHCI bind to the PsaF side, and a heterodimer of LHCA2 and LHCA9 associates with the PSAG and PSAH side of the PSI core complex (Huang et al., 2021; Ozawa et al., 2018; Suga et al., 2019). LHCA3 binds at the PSAK side and is unstable in the absence of PSI core complex, whereas the other LHCIs (LHCA1-2/4-9) are stable in the absence of PSI core complex (Naumann et al., 2005; Ozawa et al., 2018; Takahashi et al., 1991, 2004). Accordingly, it is inferred that the instability of Chls$_{GG}$-containing LHCA3 in the light is mainly caused by the instability of the Chl a_{GG}-containing PSI core complex in the light. It is inferred that LHC complexes are structurally more flexible than PSI and PSII core complexes.

Possible involvement of LHL3-GGR complex in chlorophyll-protein complex assembly

In the present study, we showed that LHL3 interacts with GGR (Figure 7), and the absence of LHL3 results in the destabilization of GGR (Figure 1). These findings are consistent with the results reported in plants (Tanaka et al., 2010). The primary structure of LHL3 and GGR suggests that LHL3 contains two putative transmembrane helices and an LHC-motif, whereas GGR is extrinsic (Figure S2). It was indicated that the LHC motif of LIL3 is required to tether GGR to the thylakoid membranes in *A. thaliana* (Takahashi et al., 2014). It was also reported that LIL3 stabilizes protochlorophyllide oxidoreductase (POR) in *A. thaliana* (Hey et al., 2017). Thus, it is speculated that LIL3 plays a role in tethering soluble enzymes to the thylakoid membranes where the assembly of chlorophyll-protein complexes takes place (Hey et al., 2017). Of interest, we detected two PSI complex assembly factors, Ycf3 and Ycf4, in the LHL3-GGR preparation by immunoblotting (Boudreau et al., 1997), although the amount of Ycf3 and Ycf4 in the LHL3-HA/GGR preparation was rather small. Figure 7 confirms the presence of LHL3 and GGR in the

purified Ycf3-HA and HA-Ycf4 preparations (Nellaepalli et al., 2018). Previously, the interaction between chlorophyll synthase, ChlG, one of the terminal enzymes of chlorophyll biogenesis, and Ycf39 protein, an assembly factor for PSII, or the YidC/Alb3 insertase, was identified (Chidgey et al., 2014). These results suggest a close interaction between chlorophyll biosynthesis and assembly of chlorophyll-binding protein complexes. Since the interaction between LHL3-GGR and the PSI complex assembly factors, Ycf3 and Ycf4, was weak, further studies are required to confirm the interaction between chlorophyll biosynthesis and assembly of reaction center complexes. The present observations are intriguing toward elucidating how Chls are integrated into chlorophyll-binding apoproteins.

MATERIALS AND METHODS

Strains and growth conditions

WT and mutant strains of *C. reinhardtii* were grown in tris-acetate-phosphate (TAP) medium (pH 7.0) at 25°C under dark or the continuous light illumination of 2–200 μmol photons m^{-2} sec^{-1} (Harris, 1989). In this study, dim light (DL) was set to 2–5 μmol photons m^{-2} sec^{-1}, medium-light (ML) to 30 μmol photons m^{-2} sec^{-1}, and high light (HL) to 200 μmol photons m^{-2} sec^{-1}. 1 μM phytol (Tokyo Chemical Industry, Tokyo) was exogenously added either in TAP liquid medium or TAP and HSM solid media as indicated. Growth test on solid media was performed by spotting 10 μL of the culture in which cells were grown to the density of mid-logarithmic phase (4×10^6 cells mL^{-1}). Genetic crosses and tetrad analysis were performed according to established methods (Harris, 1989).

Nuclear transformation

A DNA fragment carrying the *Chlamydomonas LIL3* gene (−1127 to +3928 relative to the A of the ATG start codon as +1) was amplified from *Chlamydomonas* DNA by PCR using primers #1 and #2. The *LIL3* gene flanked by promoter/5′-UTR and terminator (−1027 to +3801 relative to the A of ATG start codon as +1) was amplified from the previous PCR mixture by PCR using primers #3 and phosphorylated #4. The resulting PCR product was purified with illustra GFX PCR DNA and Gel Band Purification Kit (GE Healthcare Life Science, Buckinghamshire), digested by XhoI, and cloned into an XhoI/SmaI-digested pSL18 to generate plasmid pCS1. The pSL18 vector carries a paromomycin-resistant cassette (Depege et al., 2003). The pCS1 was digested with NotI and self-ligated to generate nuclear transformation vector pCS2. DNA segment amplified by PCR was confirmed by DNA sequencing (primers #5–#18). The primers used are listed in Table S1a,b.

Chlamydomonas nuclear transformation was carried out basically as described (Yamano et al., 2013). Briefly, cells (1 to 2×10^6 cells mL^{-1}) were harvested at 25°C and resuspended in TAP liquid medium that contained 40 mM sucrose to a final concentration of 1×10^8 cells mL^{-1}. Three microliter of 100 ng μL^{-1} ScaI-digested each transformation vector was mixed with 117 μL of the cell suspension and delivered into the cells by electroporation with Super Electroporator NEPA21 (Nepa Gene Co., Ltd., Chiba). For the vector control, ScaI-digested pSL18 was used for nuclear transformation. Transformants were selected on TAP agar plate that contained 10 μg mL^{-1} paromomycin. Subsequently, putative transformants which exhibit photoautotrophic growth were selected.

The genomic region of *GGR1* in the *lhl3* mutant was amplified in several fragments and sequenced using primers KG155 through KG167 (Table S1c), and the sequence from the mutant was found to be identical to that of the WT. The coding sequence of *LHL3* was amplified by RT-PCR using primers KG184 and KG185 (Table S1d). cDNA was synthesized from 2 μg of total RNA with Omniscript (QIAGEN) following the manufacturer's instructions. Sequencing primers are listed in Table S1e. The coding sequence of *LHL3* from the mutant was found to have a 16-nucleotide deletion from position 37 to 52. The resulting transcript is predicted to translate correctly until the 12th amino acid after which it is predicted to mistranslate an additional 58 amino acids until terminating with a premature stop codon (Figure S2b). TargetP—2.0 (https://services.healthtech.dtu.dk/services/TargetP-2.0/) predicted a chloroplast transit peptide cleavage after the 27th amino acid from the WT LHL3 protein. The deletion in the *LHL3* gene was confirmed by PCR amplification of total DNA isolated from cells using a pair of primers (primers #19/20, Table S1b).

Thylakoid membrane preparation and pigment-protein complex separation

Cells grown to the density of $2–4 \times 10^6$ cells mL^{-1} were harvested by centrifugation at 3000×*g* at 25°C for 5 min, and the pellet was resuspended in 0.3 M sucrose, 25 mM HEPES-NaOH pH 7.5, 1 mM $MgCl_2$ in the presence of 1 mM PMSF, benzonase (nuclease) (Merck Millipore) and protease inhibitor cocktail, cOmplete Mini (Sigma-Aldrich). The cells were disrupted using a French pressure cell (Amicon) and then were collected by centrifugation at 15 600×*g* at 4°C for 20 min and washed with 0.3 M sucrose, 5 mM HEPES-NaOH pH 7.5, 10 mM EDTA. The pellet (crude membrane fraction) was resuspended in a buffer containing 1.8 M sucrose, 5 mM HEPES-NaOH pH 7.5, 10 mM EDTA and was transferred to an ultracentrifuge tube. The crude membrane fraction was overlaid by 1.3 M sucrose, 5 mM HEPES-NaOH pH 7.5, 10 mM EDTA and 0.5 M sucrose, 5 mM HEPES-NaOH pH 7.5, 10 mM EDTA, and was centrifuged at 202 000×*g* at 4°C for 1 h. The floated thylakoid membranes in the layer containing 1.3 M sucrose, 5 mM HEPES-NaOH pH 7.5, 10 mM EDTA were collected and were suspended with the solution of 5 mM HEPES, pH 7.6, 10 mM EDTA as described previously (Chua & Bennoun, 1975; Takahashi et al., 1991). Thylakoid membranes (800 μg Chl mL^{-1}) were solubilized with 1% (w/v) *n*-dodecyl-β-D-maltoside (β-DDM) or *n*-dodecyl-α-D-maltoside (α-DDM), and the extracts were subjected to sucrose density ultracentrifugation for the separation of pigment-protein complexes as described previously (Takahashi et al., 2006).

Affinity purification of HA-tagged proteins

The thylakoid membranes containing 100 μg Chl mL^{-1} were solubilized with 1% (w/v) α-DDM and the extracts were applied onto a spin-column. Twenty microliters of anti-HA beads (HA-tagged protein purification kit, MBL) were added to the spin-column containing the thylakoid membrane extracts, and the mixture was incubated at 4°C in an end-over-end mixer for 1 h. The flow-through was eluted out of the spin-column by centrifugation at 6800×*g* for 10 sec and the column was washed three times. HA-tagged proteins were eluted by incubating the anti-HA beads with an elution buffer containing HA peptide as described (Nellaepalli et al., 2018; Rathod et al., 2022).

SDS-PAGE, BN-PAGE, and immunoblotting

Samples were denatured in the presence of 0.1 M DTT and 2% SDS at 80°C for 3 min. The denatured proteins were separated by SDS-PAGE (Laemmli, 1970). Polypeptides were transferred to nitrocellulose membrane by electroblotting. The antibodies against PsaA, PSAD, PsaL, PsbA, PsbC, LHCII (CP26, LHCII-type I/type III/IV) and LHCI (LHCA1-LHCA9), Ycf3, Ycf4, GGR, and LHL3 were used. Antibody against LHL3 was generated using synthesized oligopeptides CGAGLIEQQESFLGKL (184–198 aa) and CYKGLIDEATFYDKQW (219–233 aa), of which cysteine residue was conjugated to the carrier protein, keyhole limpet hemocyanin (Eurogentec). For the separation of pigment-protein complexes, thylakoid membranes (100 μg Chl mL^{-1}) were solubilized with 1% (w/v) α-DDM, and the extracts were applied on Blue Native gel electrophoresis (6–10% acrylamide gradient gel) as described previously (Nellaepalli et al., 2021).

Measurements of photosynthetic activities

Chlorophyll fluorescence transients were measured by using a pulse-amplitude modulated fluorometer (Dual PAM 100, WALZ) (Onishi & Takahashi, 2009). Photooxidation of P700 in cells was analyzed by measuring absorption changes at 705 nm in the presence of 10 μM 3-(3,4-dichlorophenyl)-1,1-dimethylurea (DCMU) and 10 μM 2,5-dibromo-3-methyl-6-isopropylbenzoquinone (DBMIB) with a Joliot-type spectrophotometer (JTS-10, BioLogic, France). Cells grown in TAP medium under low light (5 μmol photons m^{-2} sec^{-1}) were resuspended in HSM medium containing 10% (w/v) Ficoll. Oxygen-evolving activity of cells grown in TAP medium was measured using a Clark-type oxygen electrode (oxytherm OXYT1; Hansatech Instruments). Cells (5 μg Chl mL^{-1}) were illuminated with an actinic light of 7000 μmol photons m^{-2} sec^{-1} in the presence of 0.3 mM 2,6-dichloro-1,4-benzoquinone (DCBQ) as an artificial electron acceptor as reported in Kuroda et al. (2014).

Analysis of stability of thylakoid membrane proteins: WT and *Ihl3* cells in TAP medium were treated with 100 μg mL^{-1} chloramphenicol or cycloheximide, an inhibitor of chloroplast translation or cytoplasmic translation, respectively, up to 6 h under ML condition.

Pigment analysis

Fifty to two hundred microliters of cells (0.1 μg Chl μL^{-1}) were centrifuged at 21 500×*g*, and the samples resuspended with water were frozen with liquid nitrogen and lyophilized. Pigments were extracted from lyophilized cells with *N,N*-dimethylformamide (DMF) (Ikeda et al., 2008). Samples were centrifuged at 21 500×*g* 4°C for 5 min, the supernatant was filtered through a PTFE filter (0.2 μm pore size) and applied onto an HPLC (ACQUITY, UPLC/PDA system; Waters) for pigment analysis.

Pigments of cells and the thylakoid membranes were also extracted with methanol, and chlorophyll concentrations were determined spectroscopically with a Hitachi spectrometer according to Porra and Grimme (1978).

AUTHOR CONTRIBUTIONS

SK and YT designed the study. SK, SN, CS, HK, KG, MK, PT, and SM performed biochemical and molecular genetics experiments. RT generated GGR antibodies and valuable suggestions. S-IO performed the analysis of pigments by HPLC. KS, NS, and YT wrote the manuscript with input from SW and KKN, and all authors approved it.

ACKNOWLEDGMENTS

This work was supported by JSPS KAKENHI Grant Number 16H06554, 21H02510, and 23H04960, and by the RECTOR program (Okayama University, Japan). Genetic analysis of the *C. reinhardtii Ihl3* mutant was supported by the US Department of Energy, Office of Science, Basic Energy Sciences, Chemical Sciences, Geosciences, and Biosciences Division under Field Work Proposal number 449B awarded to K.K.N. K.K.N. is an investigator of the Howard Hughes Medical Institute. pSL18 vector, anti-PsaA antibody, and anti-PsbA antibody were gifted by Michel Goldschmidt-Clermont, Kevin Redding, and Masahiko Ikeuchi, respectively.

CONFLICT OF INTEREST

The authors have not declared a conflict of interest.

DATA AVAILABILITY STATEMENT

Data will be made available on request.

SUPPORTING INFORMATION

Additional Supporting Information may be found in the online version of this article.

Figure S1-S5.

Tables S1–S3.

REFERENCES

Beale, S.I. (1990) Biosynthesis of the tetrapyrrole pigment precursor, δ-aminolevulinic acid, from glutamate. *Plant Physiology*, **93**, 1273–1279.

Ben-Shem, A., Frolow, F. & **Nelson, N.** (2003) Crystal structure of plant photosystem I. *Nature*, **426**, 630–635.

Boudreau, E., Takahashi, Y., Lemieux, C., Turmel, M. & **Rochaix, J.D.** (1997) The chloroplast ycf3 and ycf4 open reading frames of *Chlamydomonas reinhardtii* are required for the accumulation of the photosystem I complex. *The EMBO Journal*, **16**, 6095–6104.

Bujaldon, S., Kodama, N., Rappaport, F., Subramanyam, R., de Vitry, C., Takahashi, Y. *et al.* (2017) Functional accumulation of antenna proteins in chlorophyll *b*-less mutants of *Chlamydomonas reinhardtii*. *Molecular Plant*, **10**, 115–130.

Bujaldon, S., Kodama, N., Rathod, M.K., Tourasse, N., Ozawa, S.I., Selles, J. *et al.* (2020) The BF4 and p71 antenna mutants from *Chlamydomonas reinhardtii*. *Biochimica et Biophysica Acta*, **1861**, 148085.

Chidgey, J.W., Linhartova, M., Komenda, J., Jackson, P.J., Dickman, M.J., Canniffe, D.P. *et al.* (2014) A cyanobacterial chlorophyll synthase-HliD complex associates with the Ycf39 protein and the YidC/Alb3 insertase. *Plant Cell*, **26**, 1267–1279.

Chua, N.H. & **Bennoun, P.** (1975) Thylakoid membrane polypeptides of *Chlamydomonas reinhardtii*: wild-type and mutant strains deficient in photosystem II reaction center. *Proceedings of the National Academy of Sciences of the United States of America*, **72**, 2175–2179.

Dent, R.M., Haglund, C.M., Chin, B.L., Kobayashi, M.C. & **Niyogi, K.K.** (2005) Functional genomics of eukaryotic photosynthesis using insertional mutagenesis of *Chlamydomonas reinhardtii*. *Plant Physiology*, **137**, 545–556.

Depege, N., Bellafiore, S. & **Rochaix, J.D.** (2003) Role of chloroplast protein kinase Stt7 in LHCII phosphorylation and state transition in Chlamydomonas. *Science*, **299**, 1572–1575.

Devitry, C. & **Wollman, F.A.** (1988) Changes in phosphorylation of thylakoid membrane proteins in light-harvesting complex mutants from *Chlamydomonas reinhardtii*. *Biochimica et Biophysica Acta*, **933**, 444–449.

Harris, E.H. (1989) *The Chlamydomonas sourcebook: a comprehensive guide to biology and laboratory use*. San Diego: Academic Press.

Heinnickel, M., Kim, R.G., Wittkopp, T.M., Yang, W., Walters, K.A., Herbert, S.K. *et al.* (2016) Tetratricopeptide repeat protein protects photosystem I from oxidative disruption during assembly. *Proceedings of the National Academy of Sciences of the United States of America*, **113**, 2774–2779.

Hey, D., **Rothbart, M.**, **Herbst, J.**, **Wang, P.**, **Muller, J.**, **Wittmann, D. *et al.*** (2017) LIL3, a light-harvesting complex protein, links terpenoid and tetrapyrrole biosynthesis in *Arabidopsis thaliana*. *Plant Physiology*, **174**, 1037–1050.

Huang, Z., **Shen, L.**, **Wang, W.**, **Mao, Z.**, **Yi, X.**, **Kuang, T. *et al.*** (2021) Structure of photosystemI-LHCI-LHCII from the green alga *Chlamydomonas reinhardtii* in State2. *Nature Communications*, **12**, 1100.

Ikeda, Y., **Komura, M.**, **Watanabe, M.**, **Minami, C.**, **Koike, H.**, **Itoh, S. *et al.*** (2008) Photosystem I complexes associated with fucoxanthin-chlorophyll-binding proteins from a marine centric diatom, *Chaetoceros gracilis*. *Biochimica et Biophysica Acta*, **1777**, 351–361.

Inoue, S., **Ejima, K.**, **Iwai, E.**, **Hayashi, H.**, **Appel, J.**, **Tyystjarvi, E. *et al.*** (2011) Protection by α-tocopherol of the repair of photosystem II during photoinhibition in Synechocystis sp. PCC 6803. *Biochimica et Biophysica Acta*, **1807**, 236–241.

Jensen, P.E., **Haldrup, A.**, **Rosgaard, L.** & **Scheller, H.V.** (2003) Molecular dissection of photosystem I in higher plants: topology, structure and function. *Physiologia Plantarum*, **119**, 313–321.

Jordan, P., **Fromme, P.**, **Witt, H.T.**, **Klukas, O.**, **Saenger, W.** & **Krauss, N.** (2001) Three-dimensional structure of cyanobacterial photosystem I at 2.5 Å resolution. *Nature*, **411**, 909–917.

Kuroda, H., **Kodama, N.**, **Sun, X.Y.**, **Ozawa, S.** & **Takahashi, Y.** (2014) Requirement for Asn298 on D1 protein for oxygen evolution: analyses by exhaustive amino acid substitution in the green alga *Chlamydomonas reinhardtii*. *Plant & Cell Physiology*, **55**, 1266–1275.

Laemmli, U.K. (1970) Cleavage of structural proteins during the assembly of the head of bacteriophage T4. *Nature*, **227**, 680–685.

Li, C.M., **Liu, X.**, **Pan, J.H.**, **Guo, J.**, **Wang, Q.**, **Chen, C.P. *et al.*** (2019) A lil3 chlp double mutant with exclusive accumulation of geranylgeranyl chlorophyll displays a lethal phenotype in rice. *BMC Plant Biology*, **19**, 1–15.

Liu, Z.F., **Yan, H.C.**, **Wang, K.B.**, **Kuang, T.Y.**, **Zhang, J.P.**, **Gui, L.L. *et al.*** (2004) Crystal structure of spinach major light-harvesting complex at 2.72 Å resolution. *Nature*, **428**, 287–292.

Lohscheider, J.N., **Rojas-Stutz, M.C.**, **Rothbart, M.**, **Andersson, U.**, **Funck, D.**, **Mendgen, K. *et al.*** (2015) Altered levels of LIL3 isoforms in Arabidopsis lead to disturbed pigment-protein assembly and chlorophyll synthesis, chlorotic phenotype and impaired photosynthetic performance. *Plant, Cell & Environment*, **38**, 2115–2127.

Maeda, H. & **DellaPenna, D.** (2007) Tocopherol functions in photosynthetic organisms. *Current Opinion in Plant Biology*, **10**, 260–265.

Michel, H., **Tellenbach, M.** & **Boschetti, A.** (1983) A chlorophyll *b*-less mutant of *Chlamydomonas reinhardtii* lacking in the light-harvesting chlorophyll *ab*-protein complex but not in its apoproteins. *Biochimica et Biophysica Acta*, **725**, 417–424.

Moseley, J.L., **Allinger, T.**, **Herzog, S.**, **Hoerth, P.**, **Wehinger, E.**, **Merchant, S. *et al.*** (2002) Adaptation to Fe-deficiency requires remodeling of the photosynthetic apparatus. *The EMBO Journal*, **21**, 6709–6720.

Moulin, M. & **Smith, A.G.** (2005) Regulation of tetrapyrrole biosynthesis in higher plants. *Biochemical Society Transactions*, **33**, 737–742.

Naumann, B., **Stauber, E.J.**, **Busch, A.**, **Sommer, F.** & **Hippler, M.** (2005) N-terminal processing of Lhca3 is a key step in remodeling of the photosystem I-light-harvesting complex under iron deficiency in *Chlamydomonas reinhardtii*. *The Journal of Biological Chemistry*, **280**, 20431–20441.

Nellaepalli, S., **Kim, R.G.**, **Grossman, A.R.** & **Takahashi, Y.** (2021) Interplay of four auxiliary factors is required for the assembly of photosystem I reaction center subcomplex. *The Plant Journal*, **106**, 1075–1086.

Nellaepalli, S., **Ozawal, S.I.**, **Kuroda, H.** & **Takahashi, Y.** (2018) The photosystem I assembly apparatus consisting of Ycf3-Y3IP1 and Ycf4 modules. *Nature Communications*, **9**, 2439.

Nelson, N. & **Yocum, C.F.** (2006) Structure and function of photosystems I and II. *Annual Review of Plant Biology*, **57**, 521–565.

Onishi, T. & **Takahashi, Y.** (2009) Effects of site-directed mutations in the chloroplast-encoded ycf4 gene on PSI complex assembly in the green alga *Chlamydomonas reinhardtii*. *Plant & Cell Physiology*, **50**, 1750–1760.

Ozawa, S.I., **Bald, T.**, **Onishi, T.**, **Xue, H.D.**, **Matsumura, T.**, **Kubo, R. *et al.*** (2018) Configuration of ten light-harvesting chlorophyll a/b complex I subunits in *Chlamydomonas reinhardtii* photosystem I. *Plant Physiology*, **178**, 583–595.

Picaud, A. & **Dubertret, G.** (1986) Pigment protein complexes and functional properties of tetratype resulting from crosses between CP1 and CP2 less Chlamydomonas mutants. *Photosynthesis Research*, **7**, 221–236.

Porra, R.J. & **Grimme, L.H.** (1978) Tetrapyrrole biosynthesis in algae and higher plants: a discussion of the importance of the 5-aminolaevulinate synthase and dioxovalerate transaminase pathways in the biosynthesis of chlorophyll. *The International Journal of Biochemistry*, **9**, 883–886.

Qin, X.C., **Suga, M.**, **Kuang, T.Y.** & **Shen, J.R.** (2015) Structural basis for energy transfer pathways in the plant PSI-LHCI supercomplex. *Science*, **348**, 989–995.

Rathod, M.K., **Nellaepalli, S.**, **Ozawa, S.I.**, **Kuroda, H.**, **Kodama, N.**, **Bujaldon, S. *et al.*** (2022) Assembly apparatus of light-harvesting complexes: identification of Alb3.1-cpSRP-LHCP complexes in the green alga *Chlamydomonas reinhardtii*. *Plant & Cell Physiology*, **63**, 70–81.

Rudiger, W. (1997) Chlorophyll metabolism: from outer space down to the molecular level. *Phytochemistry*, **46**, 1151–1167.

Rudiger, W., **Oster, U.**, **Schoch, S.**, **Klement, H.** & **Helfrich, M.** (1998) The last steps of chlorophyll biosynthesis. *Photosynthesis: Mechanisms and Effects*, **I-V**, 3203–3208.

Shen, L.L., **Huang, Z.H.**, **Chang, S.H.**, **Wang, W.D.**, **Wang, J.F.**, **Kuang, T.Y. *et al.*** (2019) Structure of a $C_2S_2M_2N_2$-type PSII-LHCII supercomplex from the green alga *Chlamydomonas reinhardtii*. *Proceedings of the National Academy of Sciences of the United States of America*, **116**, 21246–21255.

Sheng, X., **Watanabe, A.**, **Li, A.J.**, **Kim, E.**, **Song, C.H.**, **Murata, K. *et al.*** (2019) Structural insight into light harvesting for photosystem II in green algae. *Nature Plants*, **5**, 1320–1330.

Shpilyov, A.V., **Zinchenko, V.V.**, **Grimm, B.** & **Lokstein, H.** (2013) Chlorophyll phytylation is required for the stability of photosystems I and II in the Cyanobacterium sp. PCC 6803. *The Plant Journal*, **73**, 336–346.

Shpilyov, A.V., **Zinchenko, V.V.**, **Shestakov, S.V.**, **Grimm, B.** & **Lokstein, H.** (2005) Inactivation of the geranylgeranyl reductase (ChlP) gene in the cyanobacterium Synechocystis sp. PCC 6803. *Biochimica et Biophysica Acta*, **1706**, 195–203.

Su, X., **Ma, J.**, **Pan, X.**, **Zhao, X.**, **Chang, W.**, **Liu, Z. *et al.*** (2019) Antenna arrangement and energy transfer pathways of a green algal photosystem-I-LHCI supercomplex. *Nature Plants*, **5**, 273–281.

Su, X.D., **Ma, J.**, **Wei, X.P.**, **Cao, P.**, **Zhu, D.J.**, **Chang, W.R. *et al.*** (2017) Structure and assembly mechanism of plant $C_2S_2M_2$-type PSII-LHCII supercomplex. *Science*, **357**, 816–820.

Suga, M., **Ozawa, S.I.**, **Yoshida-Motomura, K.**, **Akita, F.**, **Miyazaki, N.** & **Takahashi, Y.** (2019) Structure of the green algal photosystem I supercomplex with a decameric light-harvesting complex I. *Nature Plants*, **5**, 626–636.

Takahashi, H., **Iwai, M.**, **Takahashi, Y.** & **Minagawa, J.** (2006) Identification of the mobile light-harvesting complex II polypeptides for state transitions in *Chlamydomonas reinhardtii*. *Proceedings of the National Academy of Sciences of the United States of America*, **103**, 477–482.

Takahashi, K., **Takabayashi, A.**, **Tanaka, A.** & **Tanaka, R.** (2014) Functional analysis of light-harvesting-like protein 3 (LIL3) and its light-harvesting chlorophyll-binding motif in Arabidopsis. *The Journal of Biological Chemistry*, **289**, 987–999.

Takahashi, Y., **Goldschmidt-Clermont, M.**, **Soen, S.Y.**, **Franzen, L.G.** & **Rochaix, J.D.** (1991) Directed chloroplast transformation in *Chlamydomonas reinhardtii*: insertional inactivation of the psaC gene encoding the iron sulfur protein destabilizes photosystem I. *The EMBO Journal*, **10**, 2033–2040.

Takahashi, Y., **Yasui, T.A.**, **Stauber, E.J.** & **Hippler, M.** (2004) Comparison of the subunit compositions of the PSI-LHCI supercomplex and the LHCI in the green alga *Chlamydomonas reinhardtii*. *The Biochemist*, **43**, 7816–7823.

Tanaka, A., **Ito, H.**, **Tanaka, R.**, **Tanaka, N.K.**, **Yoshida, K.** & **Okada, K.** (1998) Chlorophyll a oxygenase (CAO) is involved in chlorophyll b formation from chlorophyll a. *Proceedings of the National Academy of Sciences of the United States of America*, **95**, 12719–12723.

Tanaka, R., **Oster, U.**, **Kruse, E.**, **Rudiger, W.** & **Grimm, B.** (1999) Reduced activity of geranylgeranyl reductase leads to loss of chlorophyll and tocopherol and to partially geranylgeranylated chlorophyll in transgenic tobacco plants expressing antisense RNA for geranylgeranyl reductase. *Plant Physiology*, **120**, 695–704.

Tanaka, R., **Rothbart, M.**, **Oka, S.**, **Takabayashi, A.**, **Takahashi, K.**, **Shibata, M. *et al.*** (2010) LIL3, a light-harvesting-like protein, plays an essential role in chlorophyll and tocopherol biosynthesis. *Proceedings of the*

National Academy of Sciences of the United States of America, **107**, 16721–16725.

Tanaka, R. & **Tanaka, A.** (2007) Tetrapyrrole biosynthesis in higher plants. *Annual Review of Plant Biology*, **58**, 321–346.

Teramoto, H., **Itoh, T.** & **Ono, T.** (2004) High-intensity-light-dependent and transient expression of new genes encoding distant relatives of light-harvesting chlorophyll-a/b proteins in *Chlamydomonas reinhardtii*. *Plant & Cell Physiology*, **45**, 1221–1232.

Umena, Y., **Kawakami, K.**, **Shen, J.R.** & **Kamiya, N.** (2011) Crystal structure of oxygen-evolving photosystem II at a resolution of 1.9 Å. *Nature*, **473**, 55–U65.

von Wettstein, D., **Gough, S.** & **Kannangara, C.G.** (1995) Chlorophyll biosynthesis. *Plant Cell*, **7**, 1039–1057.

Wei, X.P., **Su, X.D.**, **Cao, P.**, **Liu, X.Y.**, **Chang, W.R.**, **Li, M.** ***et al.*** (2016) Structure of spinach photosystem II-LHCII supercomplex at 3.2 Å resolution. *Nature*, **534**, 69–74.

Yamano, T., **Iguchi, H.** & **Fukuzawa, H.** (2013) Rapid transformation of *Chlamydomonas reinhardtii* without cell-wall removal. *Journal of Bioscience and Bioengineering*, **115**, 691–694.

Zouni, A., **Witt, H.T.**, **Kern, J.**, **Fromme, P.**, **Krauss, N.**, **Saenger, W.** ***et al.*** (2001) Crystal structure of photosystem II from *Synechococcus elongatus* at 3.8 Å resolution. *Nature*, **409**, 739–743.